Response to Referee #1 comment (RC1)

We would like to thank the reviewers for taking the time to review our manuscript and providing constructive comments. Please see our responses to the comments below.

RC1:

Summary

Yoshikai et al. provide a novel modeling study to understand and predict mangrove forest dynamics across a soil salinity gradient. The study added a plant hydraulic module, dynamic allocation module, and nutrient (nitrogen) limitation on growth into SEIB-DGVM. The new model allows for consideration of soil salinity effects on plant ecophysiology as well as soil nutrient levels in mangrove forests. After calibration of two parameters determining allocation and stomata that are unavailable from literature, the model can well represent the spatial gradient of forest structure (mean DBH) and biomass (AGB) across a salinity gradient in a mangrove forest in Japan. Other model-data comparison is also presented. Altogether, the authors conclude that including hydraulic trade-offs and differences in the ability to deal with salinity is critical and adequate for predicting dominant forest dynamics in mangrove forests.

Comments

I really like the study, which extends the existing plant hydrodynamic modeling framework (often used and calibrated in arid/semi-arid ecosystems) to coastal saline ecosystems (also water-stressed). The idea of plant hydraulic control on mangrove forest dynamics existed for some time but the study presents a novel modeling study to evaluate the idea together with field data. Overall, the manuscript is well written and includes adequate details for understanding the model. I have three major comments about model diagnostics, which hopefully can improve the manuscript.

Response:

Thank you very much for the positive assessment and constructive comments on our manuscript. We have addressed the comments suggested by the reviewer, as follows.

RC1:

First, in my opinion, the key evidence to the manuscript's conclusion is Fig. 7&8, which shows how simulated forest structure and biomass match with observed values across the salinity gradient after only modest model tuning (2 parameters in Table 2). However, it is always more important and interesting to know why the model can reproduce the observations. What trait/parameters/processes are dominant in driving the model output. Is it salt filtration efficiency? P_{50}?, ψ_{lk}?, or β_0? I would suggest running some sensitivity tests to show what traits/parameters lead to the pattern in Fig.7 and how important is the tuning of ψ_{lk} and β_0 (their differences seem to be small). In fact, I am curious about whether salt filtration efficiency or P_{50} is more important, or maybe they have to be coordinated in the model to explain the observed pattern. Such information will make the study more useful.

Response:

We have conducted sensitivity analysis of the plant hydraulic trait parameters (ε, P_{50}, ψ_{lk}, and β_0) to see the relative importance of each parameter in reproducing the observed pattern of the forest structure across a soil salinity gradient as suggested. We specifically looked into the sensitivity of

above-ground biomass (AGB), which showed contrasting changes of the two species (*Rhizophora stylosa* and *Bruguiera gymnorrhiza*) with changes in soil salinity in the forest (as shown in Fig. 7b). Please note that to examine the sensitivity of ψ_{lk}, we changed the values of both ψ_{lk} and $\psi_{l,min}$ to keep the buffers between the two parameter values; the decrease in ψ_{lk} without decrease in $\psi_{l,min}$ may otherwise lead to the xylem water conductance more susceptible to the water potential at which stomata closes.

For the analysis, we changed the value of a target parameter of one species (either *R. stylosa* or *B. gymnorrhiza*) to the one determined for the other species which is shown in Table 2, and run the "salinity gradient simulation". To save on computational cost, we run only one simulation for each sensitivity test instead of the ensemble approach done for reproducing the forest structures as shown in Fig. 7. The omission of ensemble runs resulted in some fluctuations in AGB along the soil salinity gradient (Fig. R1). However, the fluctuations were not at a level that could affect the interpretation of the overall simulated forest structural patterns across the soil salinity gradient.

The results showed that the change in the values of the parameters ψ_{lk} and $\psi_{l,min}$ had the most impact on the simulation results. The decreases in ψ_{lk} and $\psi_{l,min}$ of *B. gymnorrhiza* to the level determined for *R. stylosa* largely increased the salt tolerance of this species and resulted in the *B. gymnorrhiza*-dominated forest even at the high soil salinity conditions (i.e., > 34 ‰) (Fig. R1f). On the other hand, the increase in these parameters for *R. stylosa* to the level of *B. gymnorrhiza* reduced the salt stress tolerance of *R. stylosa* and resulted in the unsuccessful growth of this species even at the soil salinity higher than 30 ‰ where *R. stylosa* starts to dominate in the forest (Fig. R1e). These results indicate that the mangroves capacity in reducing the leaf water potential is one of the most important functional traits characterizing their salt tolerance as suggested by Reef and Lovelock (2015). The response of AGB to changes in ψ_{lk} also indicates the substantial impact of biomass allocation dynamics determined by ψ_{lk} on plant productivity.

The parameter that have impacted the simulation results next to ψ_{lk} and $\psi_{l,min}$ was the salt filtration efficiency, ε (Figs. R1a–b). The results shown in Figs. R1a–b highlighted the benefit of partial uptake of salt and associated reduction in xylem tension of *R. stylosa* for maintaining the productivity under the relatively high soil salinity (i.e., > 32 ‰). The changes in the values of P_{50} also affected the simulation results to some extent (Figs. R1c–d). The increase in P_{50} of *B. gymnorrhiza*, which increases the vulnerability to xylem cavitation, decreased the productivity of this species, and resulted in the *R. stylosa*-dominated forest at soil salinity 30 ‰ where the two species showed the same level of AGB in the simulation result shown in Fig. 7. The decrease in P_{50} of *R. stylosa* increased the AGB of this species by around 15 Mg ha^{-1} compared to the case shown in Fig. 7. While the model demonstrated the relatively high sensitivities to these parameters (ε and P_{50}), it is considered that these are the coordinated functional traits, i.e., the lower cavitation resistance (as indicated by higher P_{50} of *R. stylosa*) may result from incomplete salt removal (as indicated by higher ε of *R. stylosa*) that reduces xylem tension required to maintain water uptake (Jiang et al., 2017). Therefore, they may have to be defined as coordinated plant functional traits resulted from adaptation to salt stress in the model.

The sensitivity of AGB to b_0 turned out to be quite low suggesting that the choice of -0.6 for b_0 already leads to efficient stomatal openings for photosynthesis compared to the case of -0.4 for b_0 (Fig. R1g–h). This may explain the small variations in the leaf-level photosynthetic rates between the two species and among the different soil salinity levels, which are shown in Fig. R2d and Figs. R3a and d, respectively. Understanding the mangroves stomatal behavior relative to soil salinity and associated regulation in photosynthesis has not been well established from field data as discussed by Perri et al. (2019). Further field-based studies and implementation to the model are needed for better

representation of mangroves' stomatal conductance and associated regulation of photosynthesis under salt stress.

As an action for manuscript revision, we will include Fig. R1 in the Supporting Information, and the condensed version of the above descriptions on sensitivity analysis methodology and interpretations of the results in the method and discussion sections, respectively.

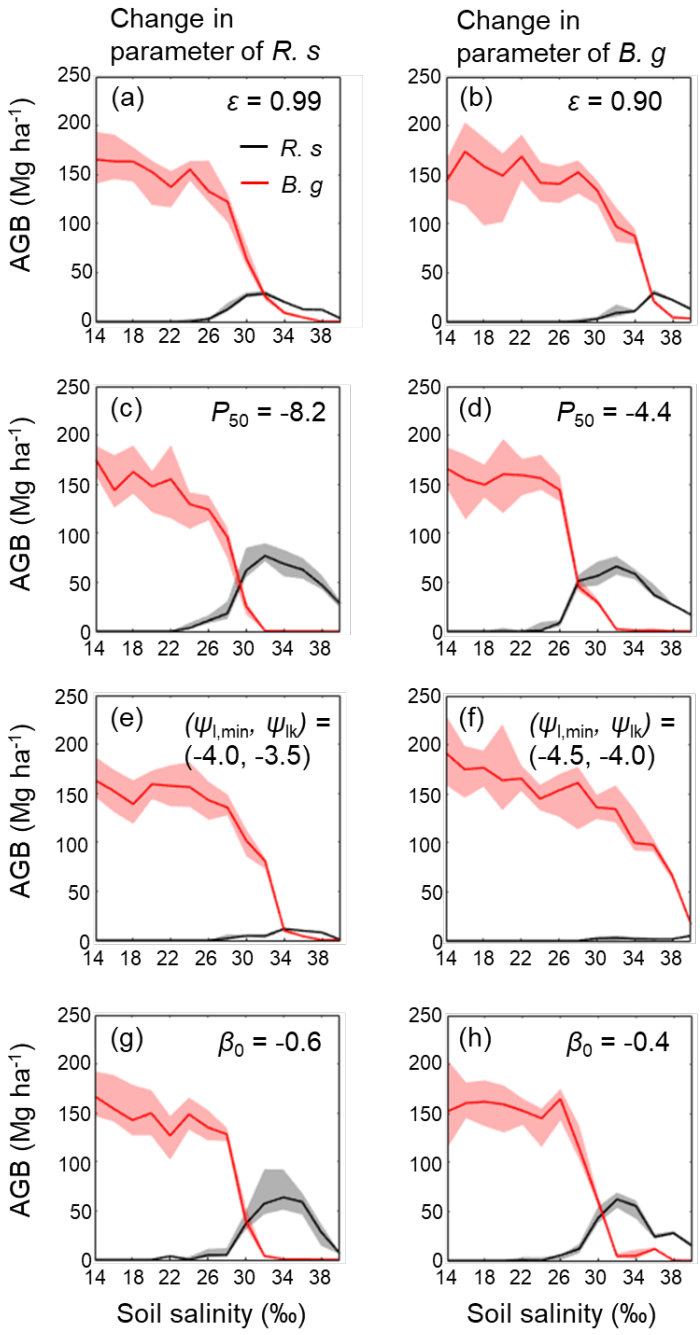

Figure R1: Sensitivity of above-ground biomass (AGB) of *R. stylosa* (*R. s*) and *B. gymnorrhiza* (*B. g*) across a soil salinity gradient to changes in parameter values of plant hydraulic traits: sensitivity to (a, b) salt filtration efficiency (ε), (c, d) water potential at which 50% of xylem conductivity is lost (P_{50}), (e, f) critical leaf water potential (ψ_{lk}) and minimum leaf water potential ($\psi_{l,min}$), and (g, h) sensitivity of marginal water use efficiency to leaf water potential (β_0). Sensitivities were examined by changing a value of one species (*R. s* or *B. g*) to the one determined for the other species shown in Table 2. Median

(solid line) and 90th percentile (shading) of AGB in steady states (> 300 years) are shown; the results are from one simulation without the ensemble approach.

RC1:
Second, compared with the plant hydraulics-salinity interaction, the efficacy of two other new modules - dynamic allocation and nutrient limitation is not well demonstrated. For example, Fig. 9 shows the huge plasticity of allometry in the model without much support from empirical data. Fig. S1 seems to suggest the allometric plasticity is observed but it is really hard to relate. Meanwhile, Fig.5 shows that including a more realistic DIN gradient did not improve the model results. Consider either including some more empirical supports or make them less central to the manuscript.

Response:

We admit that the simulated morphological traits and plasticity have not been sufficiently supported by observed data. The data shown in Fig. 9 (Comley and Mcguiness, 2005 and Komiyama et al., 2005) are the only data that we could find, and therefore we would like to make these results less central to the manuscript as suggested. Alternatively, we would like to keep the model description on the biomass allocation module and nutrient limitation in the materials & methods section in the manuscript because they are necessary for understanding the model prediction of the plants' responses to salt stress. For example, the decreased productivity under increased salt stress predicted by the model is related to the change in the biomass allocation pattern in addition to the regulation of stomatal conductance; the increase in salt stress led to increased biomass allocation to the stem and roots relative to leaves (as shown in Fig. 9), and this reduced the whole-plant photosynthesis and transpiration (which is scaled to nitrogen uptake rate) and increased carbon (through the stem and root respiration and root turnover) and nitrogen (through the root turnover) cost relative to unit leaf area, thereby reducing the productivity.

As an action for manuscript revision, we will remove sentences relevant to the implications of the dynamic biomass allocation and nutrient limitation from the abstract and concluding remarks. We will also remove Section 3.4 "Modeled morphological traits and effects of soil salinity" and 4.3 "Implications of the predicted morphological traits" from the manuscript. The contents of Figure 9 will be moved to the Supporting Information and the results will be shortly discussed in Section 4.2 "Soil salinity and interspecific competition shaping the forest structural variables" as the plants' morphological responses to salt stress and associated decrease in plant productivity. We believe that the results relevant to nutrient limitation are already not in the central focus of the manuscript (the results with more realistic DIN gradient are shown in Supporting Information Fig. S5 and are discussed shortly in the manuscript L. 548–564), thus further revision regarding this aspect is not necessary.

RC1:
Third, it is strange that no outputs from the new hydraulic module (e.g. leaf water potential diurnal cycle and seasonality) is presented, which is important to show the performance of the new plant hydraulics module.

Response:

We did not include the outputs from the hydraulic module (leaf water potential dynamics) due to lack of observed data that support model outputs – data on temporal dynamics of leaf water potential and the response to changes in soil salinity are remarkably scarce in the case of mangroves.

The panels in Fig. R2 show the seasonal variations in atmospheric variables, photosynthesis, and transpiration, that are shown in Fig. 4 in the manuscript, with addition of the simulated leaf water potential (at midday and predawn), which we consider replacing Fig. 4 with for the manuscript revision. The panels in Fig. R3 show the diurnal variations of the simulated photosynthesis, transpiration, and leaf water potential of the two species during summer and winter under two different soil salinity conditions (30 ‰ and 24 ‰).

The midday leaf water potential showed seasonal variations (Fig. R2f) as with the photosynthesis and transpiration (Fig. 2d and e). Due to the partial salt uptake of *R. stylosa* (as indicated by the lower ε value of this species) that alleviates osmotic potential difference between the soil and plant, the predawn leaf water potential of *R. stylosa* was constantly higher than that of *B. gymnorrhiza* (Fig. R2f). With the combination of the lower ε, ψ_{lk}, $\psi_{l,min}$, and higher β_0 of *R. stylosa* (Table 2), this species showed larger magnitude of leaf water potential reduction and higher leaf-level transpiration rate during summer (June–August) compared to *B. gymnorrhiza* (Figs. R2e and f). Transpiration rates of both species decreased during winter (December–February), which resulted in the similar variations in midday leaf water potential of the two species. In contrast, leaf-level photosynthetic rates of the two species were at almost the same level throughout the year (Fig. R2d), suggesting that while the value of β_0 for *B. gymnorrhiza* was set to regulate stomatal conductance compared to *R. stylosa*, the stomatal regulation was not at the level that could significantly affect the photosynthetic rate.

Compared to salinity condition 24 ‰, both species showed significantly lowered leaf-level transpiration rates under salinity condition 30 ‰ especially during summer (Fig. R3b), suggesting the stomatal regulation of the transpiration and correspondingly the water (and nutrient) uptake from the soil under high soil salinity conditions. Alternatively, the decrease in leaf-level photosynthetic rates were not significant (Fig. R3a). The leaf water potential during night-time was lower when soil salinity was 30 ‰ compared to conditions when salinity was 24 ‰, due to the different osmotic potential in soil porewater, but the leaf water potential showed almost the same levels at midday during summer, which were close to the values of ψ_{lk} determined for each species (Fig. R3c). The reduction in the leaf water potential to the level of ψ_{lk} suggests the role of dynamic biomass allocation that adjusts the whole-tree transpiration demands and hydraulic conductivity in constraining the leaf water potential dynamics. In contrast, the diurnal dynamics in leaf water potential during winter showed similar magnitude of reduction of the water potential at midday between the two soil salinity conditions (Fig. R3f), suggesting that the atmospheric control on stomatal conductance and associated dynamics is more significant than the salinity control in winter.

As an action for manuscript revision, we will replace Fig. 4 with Fig. R2. We also include Fig. R3 in the manuscript after Fig. 4 (as Fig. 5). Short descriptions on the result interpretations related to the new figures (leaf water potential seasonal and diurnal dynamics with species and salinity differences) will be included in the result section. Discussions related to this revision will also be included in the discussion section.

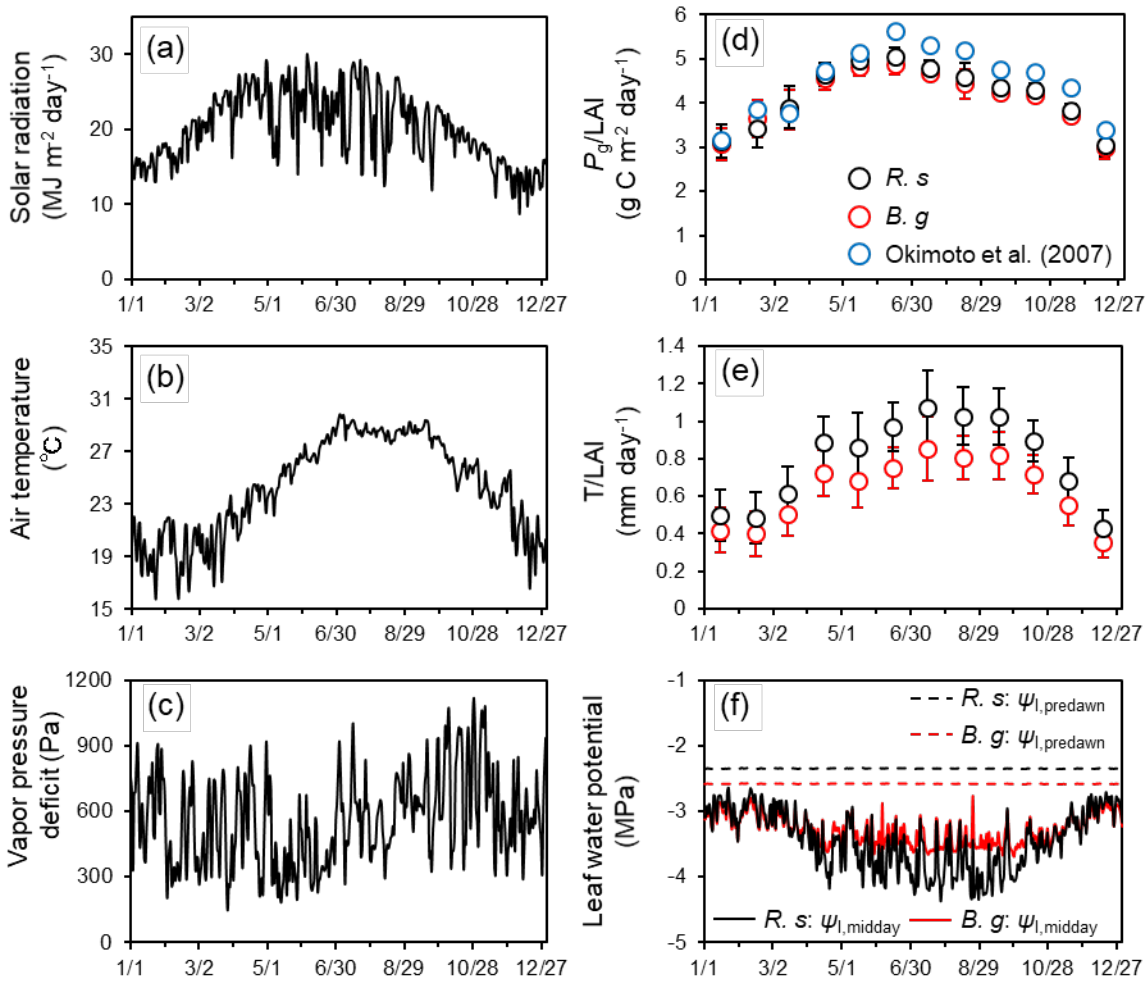

Figure R2: Seasonal variations in atmospheric forcing variables: (a) solar radiation, (b) air temperature, and (c) vapor pressure deficit (VPD), and modeled seasonal dynamics: (d) monthly mean and standard deviation of gross photosynthetic rate (P_g, g C m^{-2} ground day^{-1}) and (e) transpiration (T, mm day^{-1}) of *R. stylosa* and *B. gymnorrhiza* normalized with leaf layer index (LAI, m^2 leaf m^{-2} ground) of the respective species, and (f) midday ($\psi_{l,midday}$) and predawn ($\psi_{l,predawn}$) leaf water potential of each species. Solar radiation is expressed as daily sum while air temperature and VPD are expressed as daily mean. Leaf water potential shown is the median value of individuals. Here, the modeled dynamics were from a simulation of soil salinity set as 30‰, and the results of the year when LAI reached 1.55 are shown. During this time, the LAI of *R. stylosa* and *B. gymnorrhiza* were 0.87 and 0.68, respectively. In panel "d", the seasonal variations in GPP/LAI measured by Okimoto et al. (2007) are also shown as reference, the data of which are from an area with LAI = 1.55 in Fukido mangrove forest in 2000–2001.

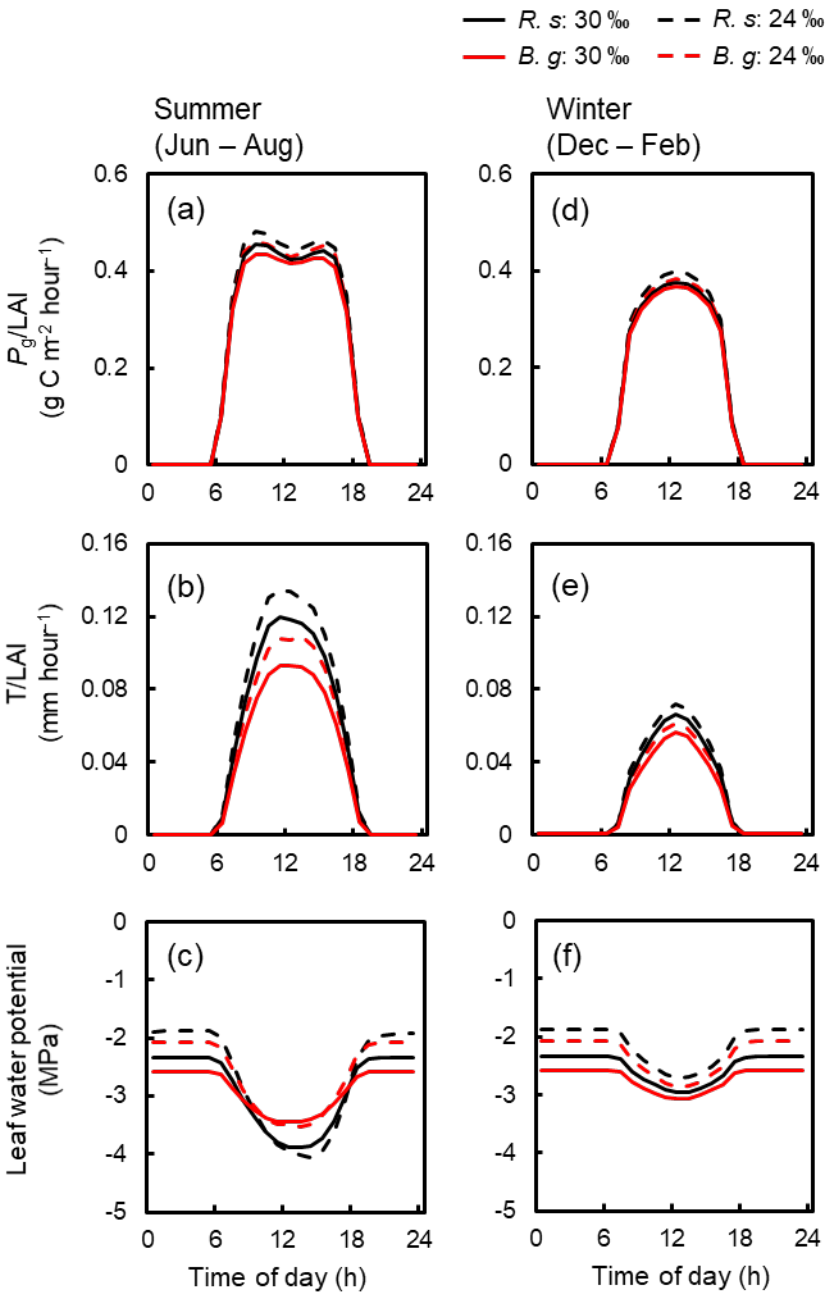

Figure R3: Simulated averaged diurnal variations in (a, d) photosynthesis and (b, e) transpiration of *R. stylosa* and *B. gymnorrhiza* normalized with LAI of the respective species, and (c, f) leaf water potential of the two species averaged for summer (June–August) and winter (December–February) under two soil salinity conditions (30 ‰ and 24 ‰). The variations under soil salinity 30 ‰ correspond to the results shown in Fig. R2. The variations under soil salinity 24 ‰ are from the results of a year that showed the same LAI (1.55). The diurnal variations in leaf water potential were derived based on the median value of individuals.

RC1: Finally, why not make the codes publicly available (line 579), especially given the new model is built on several other open-source models.

Response:

We will consider to upload the codes in GitHub and include the URL in the revised manuscript after clarifying copy rights and improving the code readability.

RC1:
Some minor comments along with the order of the text:

L. 26-27: maybe I missed it but which figure shows the self-thinning process supported by field data?

Response:
We referred to the decreasing tree density with increasing individual tree biomass patterns shown in Fig. 8 as the self-thinning process. The relevant discussions on this point can be found in L. 450–455. We will add a sentence explaining that the observed pattern in the tree density and increasing individual tree biomass is a result of the self-thinning process, which can be widely observed in mangrove forests (e.g., Deshar et al., 2012; Kamara et al., 2012; Khan et al., 2013).

RC1:
L. 120. Figure 1a, please use Mainland China or Fujian (the province) when all the other names are at province/prefecture level

Response:
We will correct the Figure 1a. Thank you for pointing it out.

RC1:
L. 171. Fig. 2 I remembered most physiological processes use daily time steps in the original SEIB-DGVM? So the photosyntheis module was rewritten to hourly time step in this study?

Response:
Yes, the photosynthesis model in SEIB-DGVM was replaced with the leaf flux model of Bonan et al. (2014) and photosynthesis was simulated with hourly time step in this study. The relevant descriptions can be found in L. 205–212 in the method section. The descriptions on the adaptation of the leaf flux model of Bonan et al. (2014) in this study have been provided in Note S4 in the Supporting Information.

RC1:
L. 184-186. I am not an expert on hydraulics in saline waters but is the osmotic potential also determined by temperature?

Response: Yes, the osmotic potential is also a function of (porewater) temperature. However, please note that sensitivity of the osmotic potential to change in temperature is significantly small compared to salinity because the osmotic potential is expressed using the temperature unit of Kelvin as described below. In this study, the osmotic potential in the soil (ψ_π, MPa) was computed using the following equation, which was adopted from Perri et al. (2019)

$$\psi_\pi = -CRi_v T_w \times 10^{-6}$$

where, C is the salt concentration (mol m^{-3}), R is the universal gas constant (J K^{-1} mol^{-1}), i_v is the van't Hoff coefficient, and T_w is the water temperature (K). Assuming that NaCl is the dominant solute, C is given by $C = sal \times \rho_w / 58.44$, where sal is the salinity of porewater expressed in ‰, ρ_w is the water

density (kg m^{-3}) and i_v = 2. Because the variations in porewater temperature T_w were not solved in this study, a constant value 298.15 K was given for the computation of the osmotic potential.
As an action for manuscript, we will include a description that the constant temperature value was used for the calculation of osmotic potential.

RC1:
L. 397. I guess tree size distribution is also available? Why not compare the simulated and observed size distribution in addition to mean DBH (maybe in supplementary)

Response:
Yes, the tree size distribution is available from the model outputs, however, the comparison with field data is complicated. Tree size distributions vary even at the same salinity condition, as implied from Fig. 7a of the variations in the mean DBH at the same salinity levels; thus, it is difficult to determine a representative tree size distribution for a given salinity condition from the field data. Therefore, a fair comparison of tree distribution between the model and data along with the salinity gradient is difficult. Alternatively, we believe that the comparisons for the mean DBH, AGB, and tree density–mean individual AGB relationship (Figs. 7 and 8) provide a sufficient assessment of model reproducibility of the forest structures along the soil salinity gradient.

RC1:
L. 405. Fig. 8. It seems the model generally underestimates tree density? Any explanations?

Response:
Yes, the model unfortunately underestimated tree density specifically in salinity conditions higher than 30 ‰ where *R. stylosa* starts to dominate as seen in the Fig. 8. We consider that this was because of the prescribed DBH-maximum crown diameter (D^*_{crown}) allometric relationship of *R. stylosa* shown in Fig. S1, which generally gives larger D^*_{crown} compared to observed values for this species. The crown diameters of individuals basically determine the tree accommodation spaces, and therefore the overestimated crown diameter may have resulted in the underestimation of the tree density. Please see Supporting Information L. 29–45 for the reason of choice of the DBH-D^*_{crown} relationship for *R. stylosa*. We expect that giving more realistic DBH-D^*_{crown} relationship for *R. stylosa* will improve the model prediction, and this could be addressed in future studies. A short discussion on this point has been provided in L. 455–460.
As an action for manuscript revision, we will add an explanation of the reason of the underestimation of tree density.

References

Bonan, G. B., Williams, M., Fisher, R. A., & Oleson, K. W. (2014). Modeling stomatal conductance in the earth system: linking leaf water-use efficiency and water transport along the soil–plant–atmosphere continuum. Geoscientific Model Development, 7(5), 2193–2222.

Comley, B. W., & McGuinness, K. A. (2005). Above-and below-ground biomass, and allometry, of four common northern Australian mangroves. Australian Journal of Botany, 53(5), 431–436.

Deshar, R., Sharma, S., Mouctar, K., Wu, M., Hoque, A. T. M. R., & Hagihara, A. (2012). Self-thinning exponents for partial organs in overcrowded mangrove *Bruguiera gymnorrhiza* stands on Okinawa Island, Japan. Forest ecology and management, 278, 146-154.

Jiang, G. F., Goodale, U. M., Liu, Y. Y., Hao, G. Y., & Cao, K. F. (2017). Salt management strategy defines the stem and leaf hydraulic characteristics of six mangrove tree species. Tree physiology, 37(3), 389–401.

Kamara, M., Deshar, R., Sharma, S., Kamruzzaman, M. D., & Hagihara, A. (2012). The self-thinning exponent in overcrowded stands of the mangrove, *Kandelia obovata*, on Okinawa Island, Japan. Journal of oceanography, 68(6), 851-856.

Khan, M. N. I., Sharma, S., Berger, U., Koedam, N., Dahdouh-Guebas, F., & Hagihara, A. (2013). How do tree competition and stand dynamics lead to spatial patterns in monospecific mangroves?. Biogeosciences, 10(4), 2803–2814.

Komiyama, A., Poungparn, S., & Kato, S. (2005). Common allometric equations for estimating the tree weight of mangroves. Journal of tropical ecology, 21(4), 471–477.

Perri, S., Katul, G. G., & Molini, A. (2019). Xylem–phloem hydraulic coupling explains multiple osmoregulatory responses to salt stress. New Phytologist, 224(2), 644–662.

Reef, R., & Lovelock, C. E. (2015). Regulation of water balance in mangroves. Annals of botany, 115(3), 385–395.